Shear resistance mechanics of beam-column joints under reversed cyclic loading

Shear Resistance Mechanisms of Beam-Column Joints under Reversed Cyclic Loading

Résistance au cisaillement d'assemblages poutre-colonne sous l'effet de charges cycliques inversées

Der Schubwiderstand von Stahlbetonknoten unter Wechsellast

Hiroshi NOGUCHI
Assoc. Professor
Chiba University
Chiba, Japan

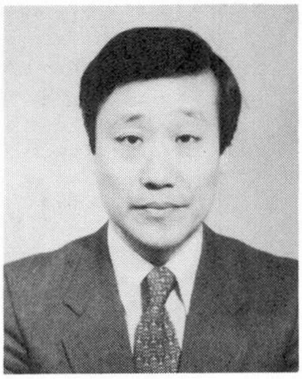

Hiroshi Noguchi, born 1946, received his doctor of engineering degree at the University of Tokyo in 1976. Since then he has been responsible for research in the application of FEM to reinforced concrete structures. He has been involved in the seismic design of reinforced concrete structures.

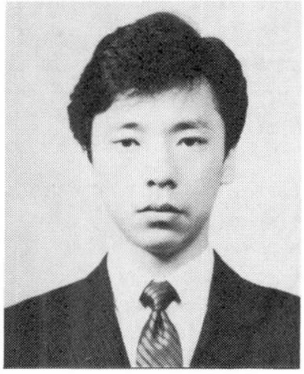

Kazuhiro Watanabe, born 1964, received his engineering bachelor's degree at Chiba Institute of Technology in 1986. Since then he has been involved in the application of FEM to reinforced concrete beam-column joints in the master course of Chiba University.

Kazuhiro WATANABE
Graduate Student
Chiba University
Chiba, Japan

SUMMARY
The nonlinear behaviour of RC beam-column joints under reversed cyclic loading was analyzed by the FEM with the emphasis on the shear resistance mechanisms of a joint. Shear forces contributed by concrete and shear reinforcing bars were calculated from the FEM analytical data. Shear forces contributed by the corresponding components of the previous macro model: the strut mechanism and truss mechanism were also calculated from the corresponding FEM analytical data. The applicability of the macro model was discussed by comparing with the shear distribution model and beam shear model.

RÉSUMÉ
Le comportement non-linéaire d'assemblages poutre-colonne en béton armé sous l'effet de charges cycliques inversées est étudié à l'aide de la méthode des éléments finis en insistant sur les mécanismes de résistance au cisaillement de l'assemblage. Les efforts tranchants dans le béton et dans l'armature sont calculés à partir de données analytiques fournies par la méthode des éléments finis. Les comportements d'étais et de fermes ont également été calculés à l'aide de la méthode des éléments finis. L'application du macro-modèle est étudiée par comparaison avec le modèle de distribution des efforts tranchants et le modèle de la poutre.

ZUSAMMENFASSUNG
Das nichtlineare Verhalten von Stahlbetonknoten zwischen Stützen und Balken unter Wechselbelastung wurde mit FE berechnet mit besonderer Berücksichtigung der Schubtragfähigkeit. Der Beitrag der Schubkräfte von Beton und Stahl wurde aus den FE-Ergebnissen berechnet. Bei den Berechnungen wurden das Streben- und das Fachwerkmodell gegenübergestellt. Die Anwendbarkeit des vorgestellten Macromodells wird diskutiert.

1. INTRODUCTION

In Japan , the Architectural Institute of Japan (AIJ) Standard for Structural Calculation of Reinforced Concrete (RC) Structures [1] does not specify a method to design a beam-column joint against shear nor bond deterioration under seismic loading mainly because most Japanese buildings are in low-rise or medium-rise range and contain large columns and earthquake damage was rarely observed in the beam-column joint [2]. Therefore, the joint is normally reinforced laterally in a manner similar to the middle part of a column. However, with the rationalization in the design, use of higher-strength materials, large-sized deformed bars and the application of the weak-beam design concept has become popular. Application to high-rise buildings has been also discussed and translated into practice. Under these present situation, the development of a rational design method for beam-column joints has become a matter of great concern.

In the ACI Building Code [3] and New Zealand RC Code [4], the provisions for beam-column joints were recently made, but they have very different view of the shear resistance mechanisms of a joint. Therefore, it is of urgent necessity to clarify the shear resistance mechanisms for the development of a rational design method for beam-column joints.

There have been many active experimental studies for beam-column joints, but it is necessary to investigate the nonlinear behaviour of beam-column joints analytically in order to clarify the shear resistance mechanisms. The number of previous analytical studies on beam-column joints is small, and the loading history in the analysis is limited to monotonic loading [5]. Therefore, in this study, the nonlinear behaviour of beam-column joints under reversed cyclic loading was analyzed by the FEM with the emphasis on the shear resistance mechanisms of a joint [6], [7], [8]. An investigating approach in this study is shown in Fig. 1. Reflecting on that previous finite element analyses have been used rather complementally for the investigation of test results, the change of stress flow in joint concrete and the progress of bond deterioration of beam longitudinal bars after beam flexural yielding are investigated from FEM analytical data in detail [9]. It is one of the most distinctive points in the FEM analysis that internal stress flow is visible, and it is rather difficult to measure the internal stress flow in the experiment. Shear forces contributed by concrete and shear reinforcing bars are calculated from the FEM analytical data. Shear forces contributed by the corresponding components of the previous macro model: the strut mechanism and truss mechanism are also calculated from the corresponding FEM analytical data, and they are compared with those which are calculated by shear distribution model and beam shear model.

2. ANALYTICAL MODELS

2.1 General

In this study, the subject of analysis was limited to the joint without lateral beams or eccentric beams, and the plane stress was assumed. In this FEM model, the rotation of principal axes and the stress-strain curves of concrete under cyclic stresses, the criterion for opening and closing of a crack and the bond stress-slip curves under cyclic stresses were considered. These analytical models are especially important in the FEM analysis of shear and bond behaviour of R/C members under reversed cyclic loading. The development process for the analytical models was written in Refs. [8].

2.2 Concrete

The linearly varying strain triangular element was used for concrete. The nonlinear constitutive law of concrete under biaxial stresses was based on the modified Darwin's orthotropic model [10] and the Kupfer's failure criteria [11]. Darwin's model was modified substantially for the rotation of the principal stress axis, because it is very important for the analysis under reversed cyclic loading. The post-crushing behaviour of concrete, the strain-softening portion of the stress-strain curve, was represented by the step-by-step releasing method of the residual stress.

2.3 Reinforcing Bars

The longitudinal bar, the stirrup and tie were represented by the bar elements. A simple bilinear model was used for the stress-strain curve.

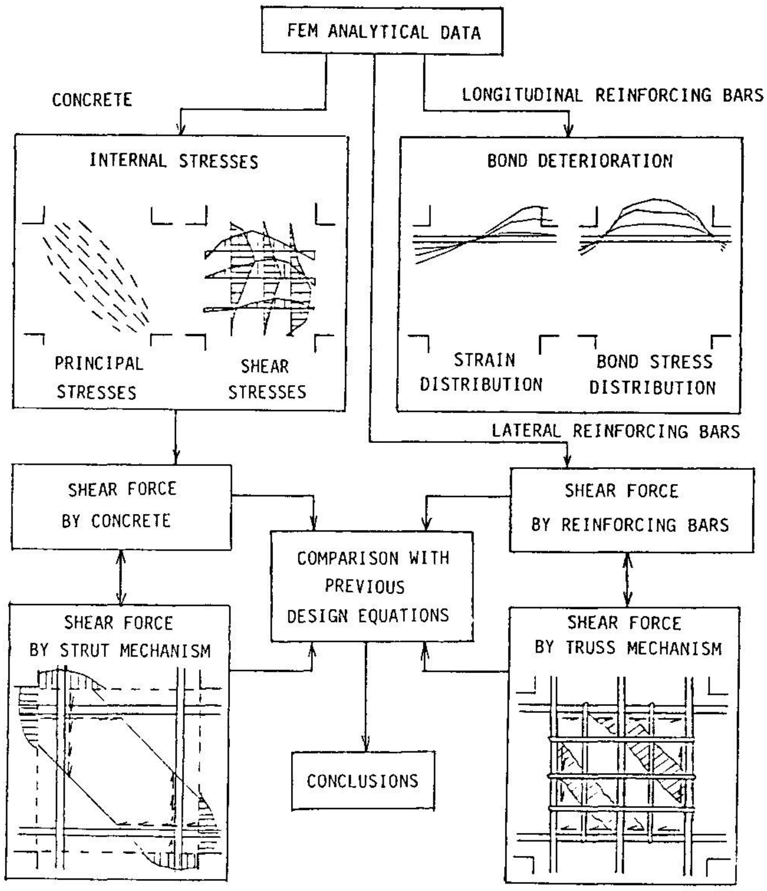

Fig. 1 Investigating Approach

2.4 Bond Slip under Reversed Cyclic Loading

Bond slip was modelled by the bond-link element. Slip characteristics parallel to the bar axis were obtained from the modified bond stress-slip curves under reversed cyclic loading, which were originally proposed by Morita and Kaku [12]. As a modified point for Morita's model, when the bond stress yielded, half of the bond stress was released and the bond stiffness was set to zero. The bond deterioration near the crack was also considered in the proposed model.

2.5 Opening and Closing of a Crack

The discrete crack model was adopted. The crack-link element was inserted between two nodes on both surfaces of a crack along the crack path which was predicted from the test results. When the principal stress at a crack nodal point exceeded the modulus of rupture, the crack is initiated by setting the spring stiffnesses both normal and parallel to the crack surface from the initial large value to zero, and the nodal forces released by the crack are applied.

When a crack was closed, the value of the spring stiffness increased gradually. The proposed model represented the following effect of the local contact of crack surfaces; as the slip parallel to the crack surface got larger, the recovery of the spring stiffness got earlier and the local contact effect came to be larger. The reopening of a crack was judged on both accumulative spring forces and principal stresses at the nodes of the crack surfaces.

2.6 Nonlinear Analytical Method

The load incremental method using the tangent modulus was adopted for the nonlinear analysis. The releasing nodal forces caused by the cracking, crushing in concrete and bond failure were applied at the next loading stage. The frontal method was used for the solution of the simultaneous, linear algebraic equations.

3. SPECIMENS FOR SUBJECTS OF ANALYSIS

Four half-scaled cross-type specimens, J - 1, J - 1', J - 2 , J - 3, were selected for the subject of analysis as shown in Table 1. The corresponding previous test results were available for the three specimens, J - 1, J - 2, J - 3. Specimen J - 1 was tested by Kamimura and Hamada [13], and specimens J - 2 and J - 3 were tested by Tada and Takeda [14]. Each specimen had its own failure mode: joint failure and bond deterioration of beam longitudinal bars (J - 1), joint failure with good bond for beam longitudinal bars (J - 1'), bond deterioration of beam bars after beam flexural yielding (J - 2), and beam flexural yielding (J - 3). It is necessary to investigate the variable failure modes affected by shear and bond derterioration for clarifying the shear resistance mechanisms in a joint. The middle longitudinal reinforcing bars were set up only in the column of J - 1' to study the role of the column middle reinforcing bars in the shear resistance of a joint with good bond for beam longitudinal bars.

The detail and the finite element idealization of interior beam-column joint specimens are shown in Figs. 2 - 3, respectively. Only half of the whole specimen was analyzed due to the symmetry of the shape and loading condition around a point. The crack pattern was set up using link elements in general accord with the test results under reversed cyclic loading. In the analysis, the specimen was loaded to the positive loading of the third cycle for J - 1, J - 2, J - 3, and to the negative peak load of the second cycle for J - 1'.

4. RESTORING FORCE CHARACTERISTICS

Table 1 Specimens for Subjects of Analysis

Specimen	J-1	J-1'	J-2	J-3
Failure Mode	Joint Failure Bond Deterioration	Joint Failure	Bond Deterioration after Beam Yielding	Beam Yielding
Bond of Beam Longitudinal Bars	Poor	Good	Poor	Perfect
Middle Longitudinal Bars of Column (SD35)	——	D-22	——	——

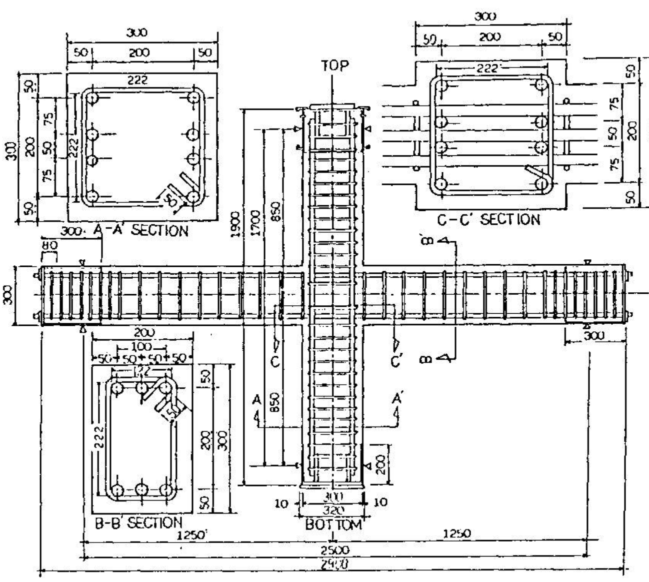

Fig. 2 Detail of Specimen

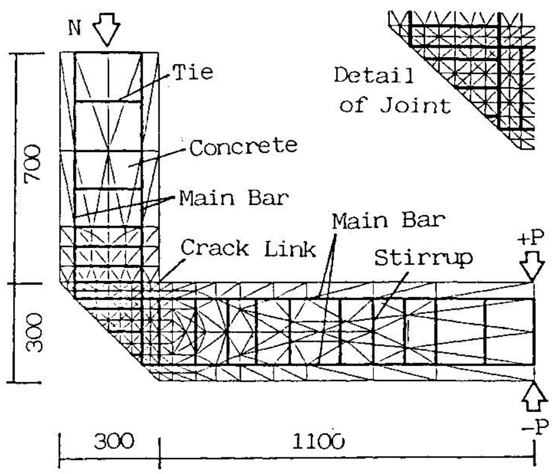

Fig. 3 Finite Element Idealization

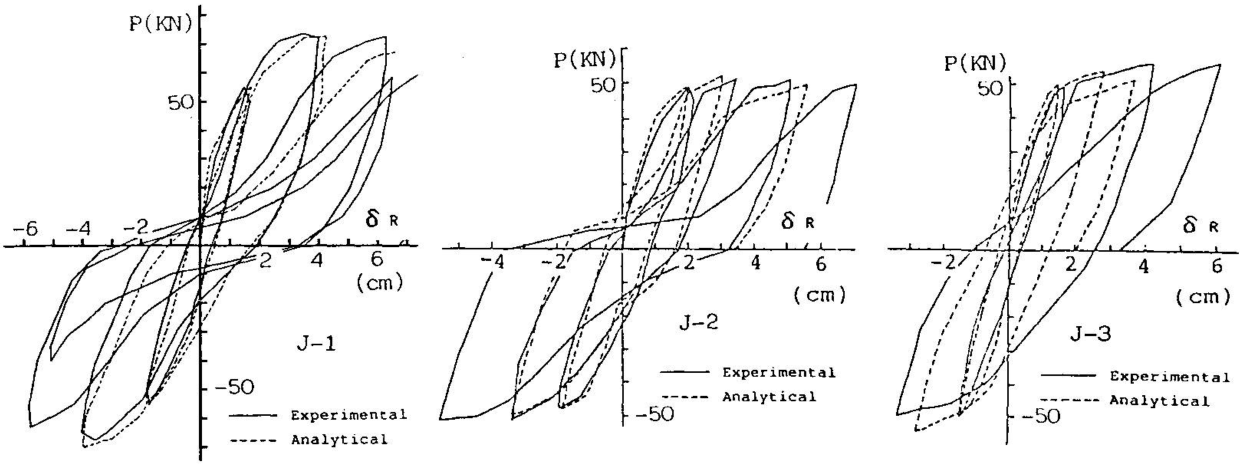

Fig. 4 Load-Story Displacement Relationships

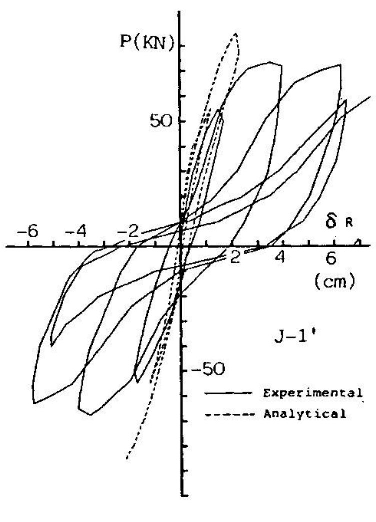

The analytical load-story displacement relationships are compared with the test results in Fig. 4. For J - 1 and J - 2, the analytical results gave good agreement with the experimental results for the shape of hysteresis loops. The analytical restoring force characteristics adopted the contra-S-shape with poor energy dissipation capacity, as cracking and bond deterioration of beam longitudinal bars in the joint progressed under the subsequent cyclic loading. This tendency was more pronounced for J - 2 in which bond deterioration became significant after yielding of beam longitudinal bars. For specimen J - 3, the analytical restoring force characteristics maintained the stable spindle-shape hysteresis loops and almost the same tendency as the test results. For specimen

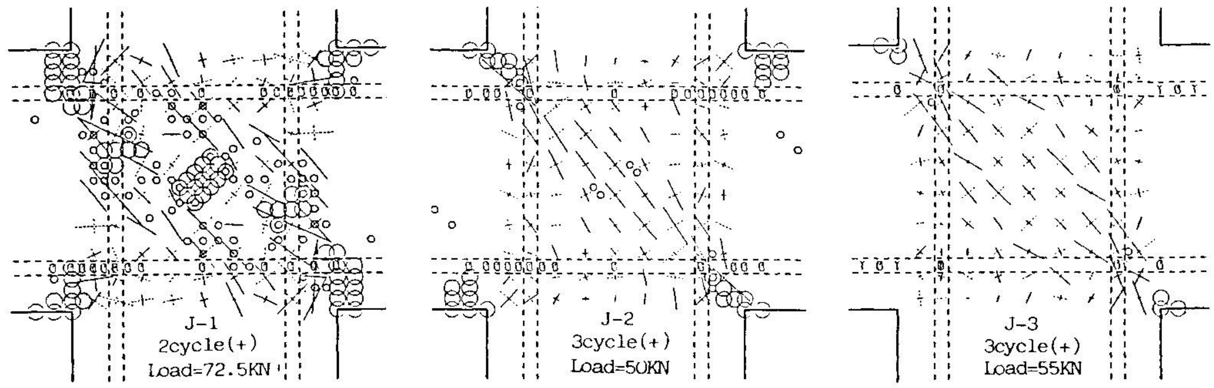

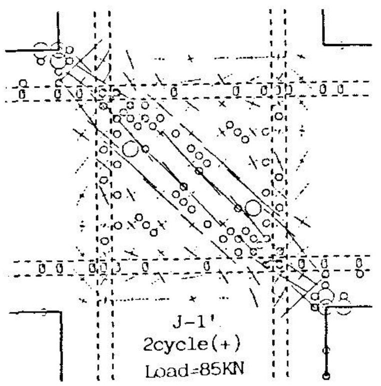

Fig. 5 Principal Stresses

J - 1' with good bond for beam longitudinal bars, the analytical maximum strength was higher than J - 1 with poor bond. The shape of hysteresis loops showed signs of the contra-S-shape at the negative load of the second cycle because of shear deterioration in the joint. The analytical results also obtained a good agreement with the test results for crack propagation, progress of failure, joint behaviour, bond slip of beam longitudinal bars through the joint and restoring force characteristics. The comparisons were discussed in Refs. [8] in detail. From those comparisons, the accuracy of the analytical results were considered to be sufficient for observing the internal stresses to investigate the shear resistance mechanisms in the joint.

5. PRINCIPAL STRESS DISTRIBUTION

Principal stress distribution in the joint concrete was shown in Fig. 5. It is one of the most distinctive points that internal stress flow is visible in FEM analysis. The compressive strut was formed along the diagonal line of the joint under near the peak load of each loading cycle. Strain-softening and compressive failure of concrete were remarkable both on the beam compression zone and along the diagonal line on the joint for J - 1. The width of compressive strut for good bond specimen, J - 3, was wider than bond deterioration type specimen, J - 2. The clear compressive strut was formed along the diagonal line for J - 1'. Strain-softening was remarkable along the diagonal line on the joint, but the compressive failure was not so remarkable as compared with J - 1.

6. SHEAR STRESSES CONTRIBUTED BY JOINT CONCRETE

The concrete shear stresses obtained by the shear distribution model were shown in Fig. 6. In the shear stress distribution model shown in Fig. 7, shear forces were obtained by subtracting the reaction forces in concrete, which were made by the truss action of shear reinforcing bars in the joint, from the integration value of the concrete shear stress over the central horizontal section in the joint. The concrete shear stresses were higher for J - 1, J - 1', joint shear failure type than J - 2, J - 3, beam flexural yielding type. The maximum shear stresses reached about 0.47 - 0.56 F_c for J - 1, J - 1'. (F_c = compressive strength of concrete) These values were corresponding to the upper bound shear stresses observed in the previous experimental studies [16]. For J - 1, the shear stress at the positive load was higher than that at the negative load for the first and second cycle. It seemed to be caused by the local compressive failure of concrete under relatively lower load. For J - 1', this tendency was not observed, because the compressive failure of concrete was not so remarkable until near the maximum strength in the second cycle. For J - 2, J - 3, the peak shear stresses kept constant values of about 0.15 F_c, and the compressive failure was not observed even after the beam flexural yielding.

The comparisons of shear stresses by joint concrete for J - 2 between the three models were shown in Fig. 7. The compressive strut mechanism model was proposed by Paulay and Park for the shear resistant component by joint concrete [15]. The concept of the beam shear model was adopted in the ACI Code. The three models obtained good agreements with the test results.

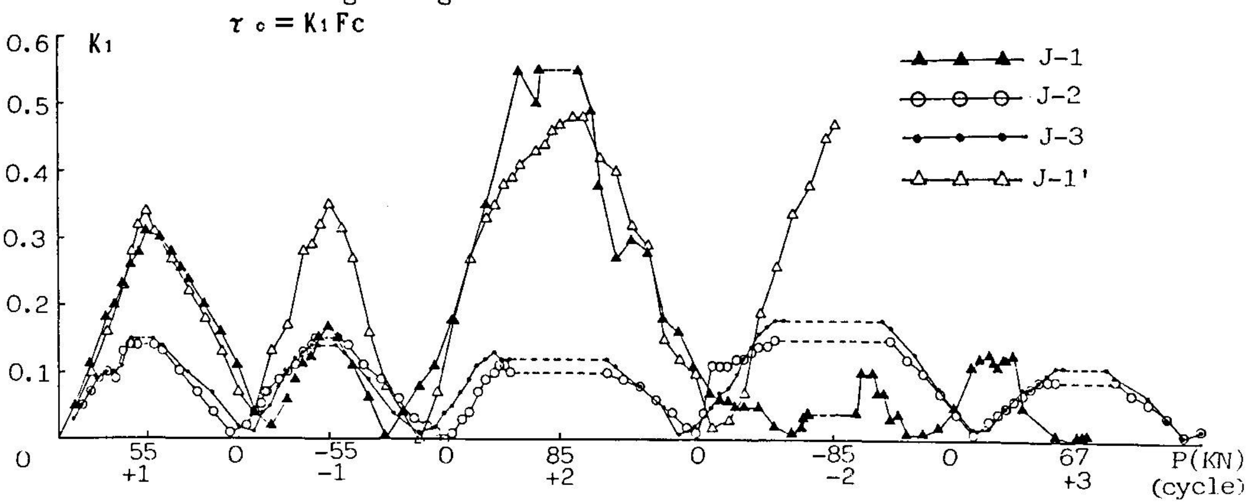

Fig. 6 Concrete Shear Stresses Calculated by Shear Distribution Model

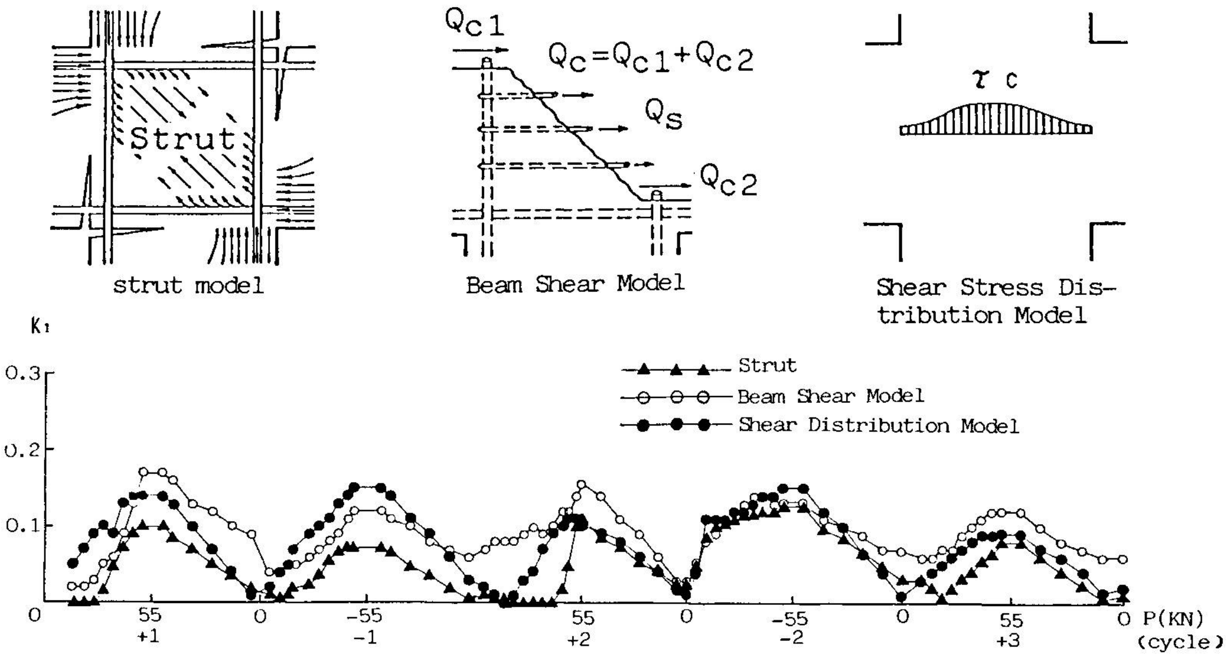

Fig. 7 Concrete Shear Stresses Calculated by Three Models

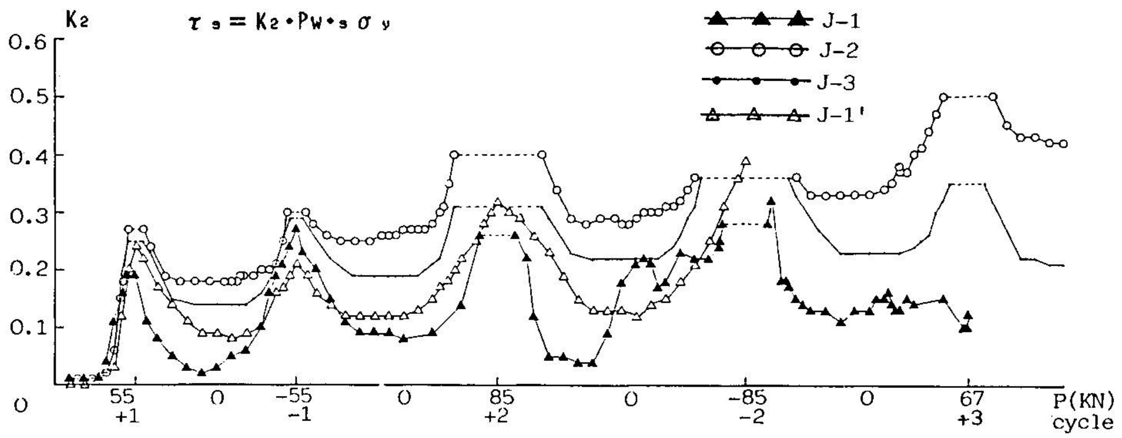

Fig. 8 Shear Stresses Contributed by Joint Reinforcing Bars

7. SHEAR STRESSES CONTRIBUTED BY JOINT REINFORCING BARS

The shear stresses, τ_s, contributed by the joint reinforcing bars were obtained from the strain in the reinforcing bars and shown as the coefficient of $p_{w\,s}\sigma_y$ in Fig. 8, in which p_w = the ratio of reinforcing bars and $_s\sigma_y$ = yielding strength of reinforcing bars. The residual stresses under lower load seemed to be caused by the local contact effect of a crack. The maximum shear forces, $\tau_{s\,max}$ were 0.33 - 0.39 $p_{w\,s}\sigma_y$ in the joint failure type, J - 1, J - 1', and 0.37 - 0.5$p_{w\,s}\sigma_y$ in the beam flexural yielding type, J - 2, J - 3. From Fig. 6 and Fig. 8, τ_c was larger for J - 3 than that for J - 2, and τ_s was larger for J - 2 than that for J - 3. Considering that p_w was the same for both specimens, it was considered that the shear forces flew into the joint mainly through the bond of beam reinforcing bars, and consequently the concrete shear stress got larger in J - 3. There was little difference between J - 1 and J - 1', but the peak shear stress increased gradually even at the second cycle for J - 1'.

8. SHEAR STRESSES CONTRIBUTED BY COMPRESSIVE STRUT MECHANISM

The macro model for the shear resistance mechanisms proposed by Park and Paulay [15] were shown in Fig. 9. In the proposed macro model, the contribution of the concrete and joint reinforcing bars to the joint shear resistance were represented by the compressive strut mechanism, and the truss mechanism, respectively. The horizontal joint shear force, V_{ch}, contributed by the compressive strut mechanism was calculated from the corresponding FEM analytical data as follows,

$$V_{ch} = {}_BC_c + \Delta\, {}_BT_c - V_{col} \qquad (1)$$

in which $_BC_c$ = horizontal concrete compression force from the beam, $\Delta\, _BT_c$ =force transferred from the beam bars to the concrete strut and V_{col} = horizontal shear force across a column (See Fig. 9). $_BC_c$ was obtained indirectly from the difference between the resultant forces of beam compressive and

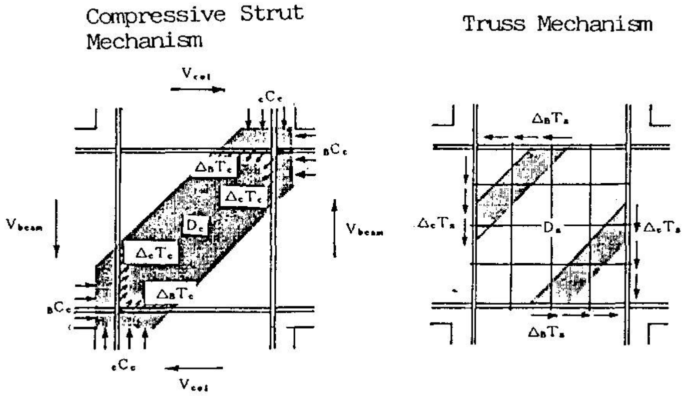

Fig. 9 Macro Model for Shear Resistance Mechanisms Proposed by Park and Paulay

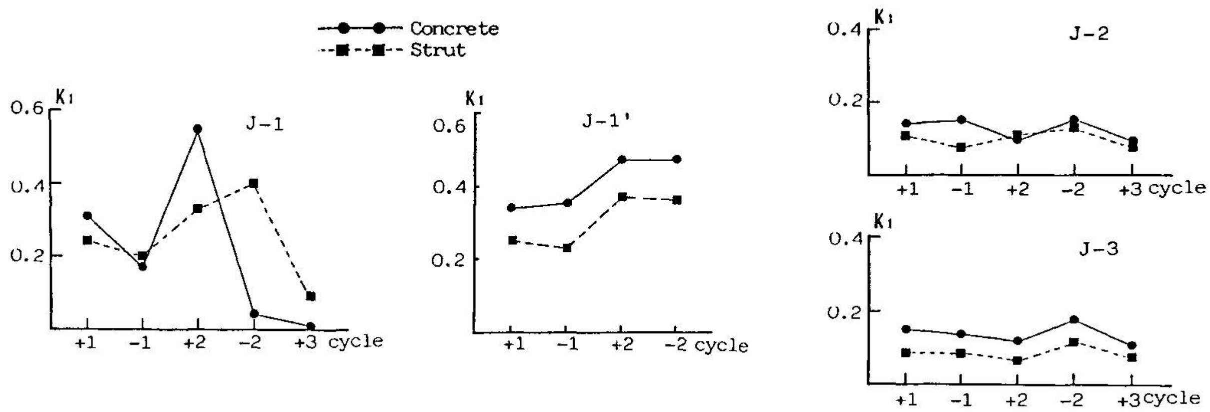

Fig.10 Concrete Shear Stresses Calculated by Strut Mechanism and Shear Stress Distribution Models

tensile longitudinal bars. The shear forces, V_{ch}, calculated by Eq. 1 were compared for the peak load in each cycle with the shear forces obtained by the shear stress distribution model in Chapter 6 in Fig. 10. The strut mechanism model gave a good agreement with the shear stress distribution model for all four specimens. It was shown that the shear stress contributed by concrete could be estimated by the compressive strut mechanism from Fig. 10 and Fig. 7.

9. SHEAR STRESSES CONTRIBUTED BY TRUSS MECHANISM

The horizontal shear forces, V_{sh}, contributed by the truss mechanism was calculated from the FEM analytical data as follows,

$$V_{sh} = \Delta_B T_s \tag{2}$$

in which $\Delta_B T_s$ = force transferred from the beam bars to the outer concrete of the strut (See Fig.9).

The shear forces, V_{sh}, calculated by Eq. 2 were compared for the peak load in each cycle with the shear forces obtained by the strain in the joint reinforcing bars in Chapter 7 in Fig. 11. The truss model was not in agreement with

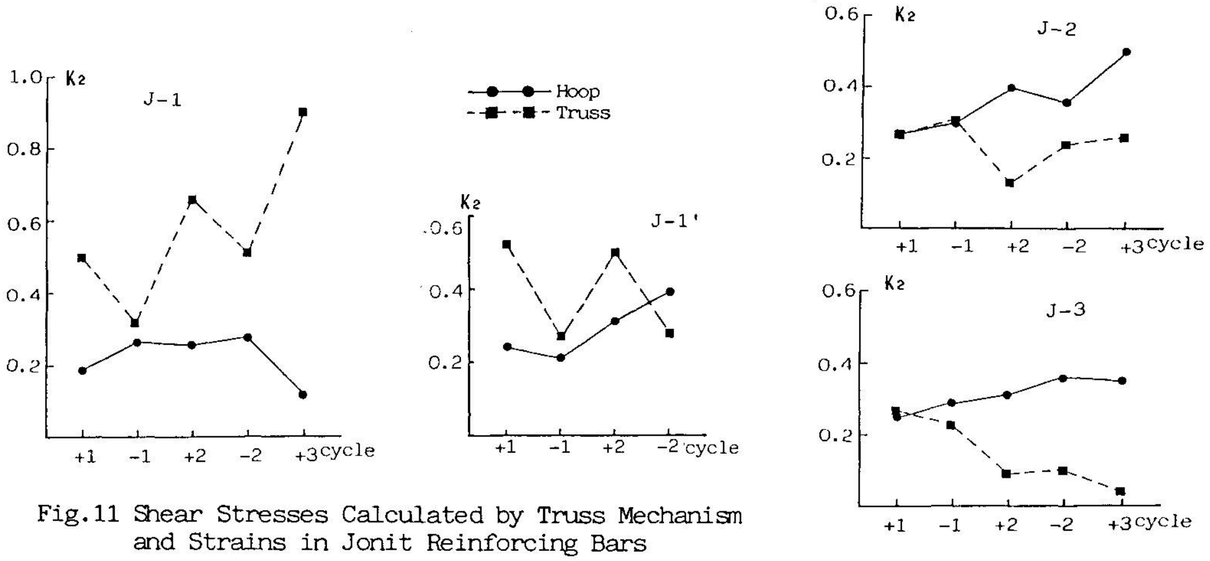

Fig.11 Shear Stresses Calculated by Truss Mechanism and Strains in Jonit Reinforcing Bars

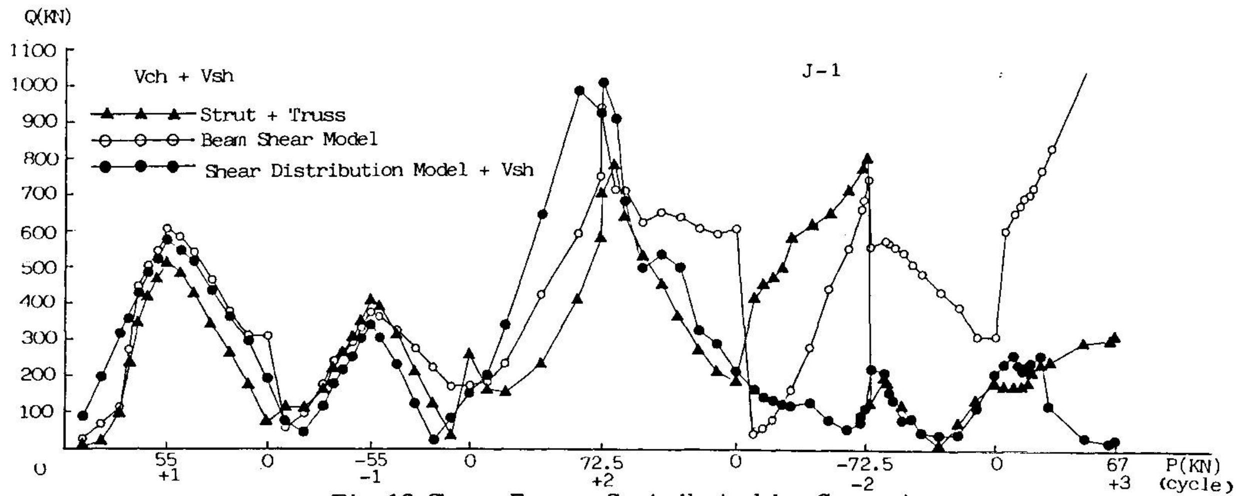

Fig.12 Shear Forces Contributed by Concrete and Joint Reinforcing Bars

the contribution of joint reinforcing bars for J - 1, J - 2, J - 3. It was considered that this was because these three specimens had no middle longitudinal bars in the column. The middle longitudinal bars in the column are considered to be necessary for forming the truss action in the proposed macro model. For J - 1' with the middle longitudinal bars in the column, the truss model gave a better agreement with the contribution of the joint reinforcing bars. For the truss model, it is considered that the further investigation is needed for the role of the middle longitudinal bars in the column and the bond forces of the beam and column longitudinal bars in the shear resistance.

10. TOTAL SHEAR FORCES CONTRIBUTED BY CONCRETE AND SHEAR REINFORCING BARS

The total of shear forces contributed by concrete and joint reinforcing bars was calculated by the three method (Figs. 6, 7) as shown in Fig. 12 for J - 1. The two mechanisms (strut and truss) model gave a good agreement with the shear stress distribution model and the beam shear model for the specimen J - 1, joint failure and bond deterioration type to the positive peak load in the second cycle. But one should note that the errors in the strut and truss mechanism were compensated each other in the two mechanism model. After the positive peak load in the second cycle, the good correspondence with the other two models could not be observed because of the local compressive failure of joint concrete.

11. INTERNAL STRESS RESULTANTS AROUND A JOINT

The vertical shear forces contributed by the strut and truss mechanisms were calculated as follows,

$$V_{cv} = {}_cC_c + \Delta {}_cT_c - V_{beam} \qquad (3)$$

$$V_{sv} = \Delta {}_cT_s \qquad (4)$$

in which V_{cv} = vertical joint shear force provided by compressive strut mechanism, V_{sv} = vertical joint shear force provided by the vertical shear reinforcing bars, ${}_cC_c$ = vertical·concrete compression force from the column, $\Delta {}_cT_c$ = force transferred from the column bars to the concrete strut, V_{beam} = vertical shear force across a beam and $\Delta {}_cT_s$ = force transferred from the column bars to the outer concrete of the strut (See Fig. 9).

The internal stress resultants around a joint combined in an equilibrium vector polygon were calculated from the FEM analytical data as shown in Fig. 13. It was shown that the concrete compression force from the beam, ${}_BC_c$, was distinguished in J - 1 and J - 2, bond deterioration type. The force transferred from the beam bars to the concrete strut, Δ_BT_c, was distinguished in J - 1' and J - 3 with good bond for beam bars.

Though the internal stress resultants around a joint were discussed qualitatively by Paulay and Park [15], it is possible to discuss quantitatively the internal stress resultants using the FEM analytical data.

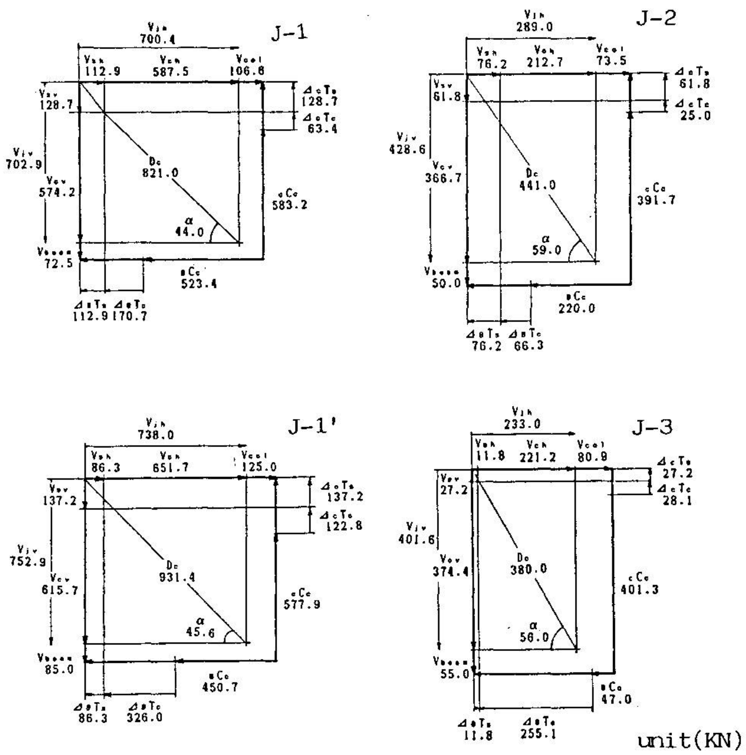

Fig.13 Internal Stress Resultants around a Joint

12. CONCLUSIONS

The nonlinear behaviour of reinforced concrete beam-column joints under reversed cyclic loading was analyzed by the FEM with the emphasis on the shear resistance mechanisms of a joint.

The maximum shear forces contributed by the joint concrete, τ_c, were 0.47 - 0.56 F_c in the joint failure type and about 0.15 F_c in the beam flexural yielding type. The shear forces contributed by joint concrete could be estimated by the compressive strut mechanism model considerably well.

The maximum shear forces contributed by the joint reinforcing bars, τ_s, were 0.33 - 0.39 $p_{ws}\sigma_y$ in the joint failure type, and 0.37 - 0.5 $p_{ws}\sigma_y$ in the beam flexural yielding type. The truss model was not in agreement with the contribution of joint reinforcing bars for the specimens without the middle longitudinal bars in the column. It was pointed out that the further investigation is needed for the role of each component of the truss model.

The investigating approach of the internal stress conditions by FEM analytical data will be one of the useful tool for the verification and development of macro model and design equations, if the systematic analysis is carried out in the further work.

REFERENCES

1. ARCHITECTURAL INSTITUTE OF JAPAN, AIJ Standard for Structural Calculation of Reinforced Concrete Structures, Sept. 1982.

2. AOYAMA, H., Problems Associated with "Weak-Beam" Design of Reinforced

Concrete Frames, ATC-15, Comparison of Building Seismic Design Practices in the United States and Japan, 1984, pp. 117-158.

3. AMERICAN CONCRETE INSTITUTE, Building Code Requirements for Reinforced Concrete Structures (ACI318-83), Detroit, 1983.

4. STANDARDS ASSOCIATION OF NEW ZEALAND, Code of Practice for the Design of Concrete Structures, NZS 3101, 1982.

5. INOUE, N. AND NOGUCHI, H., Finite Element Analysis of Reinforced Concrete in Japan, Finite Element Analysis of Reinforced Concrete Structures, Proc. of the Japan - U. S. Seminar in Tokyo, May 1985, ASCE, 1986, pp. 25-47.

6. NOGUCHI, H., Nonlinear Finite Element Analysis of Beam-Column Joints, Final Report, IABSE Colloquium on Advanced Mechanics of Reinforced Concrete, Delft, 1981, pp. 639-654.

7. NOGUCHI, H., Analytical Models for cyclic Loading of Reinforced Concrete Members, Finite Element Analysis of Reinforced Concrete Structures, Proc. of the Japan - U.S. Seminar in Tokyo, May 1985, ASCE, 1986, pp. 486-506.

8. NOGUCHI, H. and NAGANUMA, K., Nonlinear Finite Element Analysis of Restoring Force Characteristics of Reinforced Concrete Beam-Column Joints, Proc. of Eighth World Conf. on Earthquake Engrg., San Francisco, July 1984, pp. 543-550.

9. AOYAMA, H. and NOGUCHI, H., Future Prospects for Finite Element Analysis of Reinforced Concrete Structures, Finite Element Analysis of Reinforced Concrete Structures, Proc. of the Japan - U. S. Seminar in Tokyo, May 1985, ASCE, 1986, pp. 667- 681.

10. DARWIN, D. and PECKNOLD, D. A., Nonlinear Biaxial Stress-Strain Law for Concrete, Jour. Engr. Mech. Div., ASCE, Vol. 103, No.EM2, April 1977, pp. 229-241.

11. KUPFER, H. B. and GERSTLE, K. H., Behaviour of Concrete under Biaxial Stresses, Jour. Engr. Mech. Div., ASCE, Vol. 99, No.EM4, August 1973, pp. 853-866.

12. MORITA, S. and KAKU, T., Local Bond Stress-Slip Relationship under Repeated Loading, Proc. IABSE Symp., Lisbon, Portugal, Sept. 1973.

13. Kamimura, T. and Hamada, T., et al., Experimental Study on Reinforced Concrete Beam-Column Joints, Part 1-3, Proc. Annual Conv., AIJ, Sept. 1978, pp. 1673-1674, Sept. 1979, pp. 1303-1306 (in Japanese).

14. Tada, T., Takeda, T. and Takemoto, Y., Experimental Study on the Reinforcing Method of RC Beam-Column Joints, Proc. Kanto District Symp., AIJ, July 1976, pp. 225-236 (in Japanese).

15. PAULAY, T. and PARK, R., Joints in Reinforced Concrete Frames Designed for Earthquake Resistance, A Report Prepared for the U.S. - New Zealand - Japan Seminar, Monterey, California, August 1984, pp. 16-18.

16. OGURA, K. and SEKINE, M., The State of the Art of the Studies on the Reinforced Concrete Beam to Column Joint, Concrete Journal, Vol. 19, No. 9, Sept. 1981, pp. 2-15 (in Japanese).